2014 5th IEEE RAS & EMBS International Conference on
Biomedical Robotics and Biomechatronics (BioRob)
August 12-15, 2014. São Paulo, Brazil

# A Neurally Inspired Robotic Control Algorithm for Gait Rehabilitation in Hemiplegic Stroke Patients

Abhishek Mishra, Rohan Ghosh, Martina Coscia, Sunil Kukreja, *Senior Member, IEEE*, Carmelo Chisari, Silvestro Micera, *Member, IEEE*, Yu Haoyong, *Member, IEEE,* and Nitish V. Thakor, *Fellow, IEEE*

***Abstract*— Cerebrovascular accident or stroke is one of the major brain impairments that affects numerous people globally. After a unilateral stroke, sensory motor damages contralateral to the brain lesion occur in many patients. As a result, gait remains impaired and asymmetric. This paper describes and simulates a novel closed loop algorithm designed for the control of a lower limb exoskeleton for post-stroke rehabilitation. The algorithm has been developed to control a lower limb exoskeleton including actuators for the hip and knee joints, and feedback sensors for the measure of joint angular excursions. It has been designed to control and correct the gait cycle of the affected leg using kinematics information from the unaffected one. In particular, a probabilistic particle filter like algorithm has been used at the top-level control to modulate gait velocity and the joint angular excursions. Simulation results show that the algorithm is able to correct and control velocity of the affected side restoring phase synchronization between the legs.**

## I. Introduction

HEMIPARESIS after an unilateral stroke is a debilitating condition that globally affects numerous people every year. The loss of lower limb function is a traumatic outcome: it compromises individual autonomy and activities with a consequent reduction of life quality.

Rehabilitative intervention guides motor recovery, and enhances the abilities of the subjects resulting in an increase of quality of life. For post-stroke subjects, it is based on promoting and guiding the neuroplasticity in the cortex by using motor tasks in order to favor a functional recovery of gait, called the bottom-up approach [1-4]. Together with the traditional rehabilitation techniques, other innovative treatments have been introduced in the last few decades [1, 3, 5-7]. Among these methods, those employing non-invasive stimulation devices for muscles or brain have shown promising results for control of the affected limb. However, they are not suitable for long-term intervention or independent usage by patients. Alternatively, robotic rehabilitative devices provide a safe, accurate, intensive and prolonged motor therapy. In particular, robotic exoskeletons designed to deliver automated gait therapy by assisting the impaired subjects have shown encouraging results [1, 8-14].

This paper is concerned with the development and validation of an algorithm for control of a lower limb robotic exoskeleton that can predict the patient's intention to change velocity of walking. Development of advanced adaptive controls is important to improve the effectiveness of rehabilitative devices, since the performance of robotic exoskeletons depends on their control algorithms. Many such algorithms use minimization of state errors from previous iterations to control the gait [15], impedance control [16], and haptic feedback [17, 18]. However, most methods have problems adapting to patients walking with non-physiological gaits [16].

Gait models based on Central Pattern Generator (CPG) networks can generate and maintain robust rhythmic movements without continuous higher level control [19]. It has been hypothesized that CPGs constitute an important part in the neural pathway that generates and maintains a stable limit cycle behavior in bipedal gait [20-22].

In this study, we introduce a novel gait control algorithm and validate it by using data from ten hemiplegic stroke patients. The algorithm is inspired by the current holistic understanding of CPG networks in vertebrates. In particular, we use artificial neural networks with feedback to implement the CPG, and one-dimensional Self-Organizing Map (SOM) to encode and maintain a repertoire of pre-learnt basis gait behaviors [23]. Finally, the algorithm includes a probability based particle filter module for intention based velocity control. The particle filter is a probabilistic model that has been applied in robotic systems for localization [24, 25]. In this paper we use probabilities instead of particles and perform localization using SOM nodes for velocity control by the patient. We also show an analysis for the importance of promoting supraspinal initiated movements to gain complete functional recovery of the affected muscles and neural cells [26]. It is challenging to accurately predict a patient's intention to alter gait characteristics (gait transition, turning, velocity).

Nitish V. Thakor is the director of Singapore Institute of Neurotechnology (SINAPSE) and Professor of Electrical and Bioengineering at the National University of Singapore, and Professor of Biomedical Engineering at Johns Hopkins University (email: sinapsedirector@gmail.com)

Haoyong Yu is with SINAPSE and the Department of Bioengineering, National University of Singapore, 9 Engineering Drive 1, Singapore 117575 (email: bieyhy@nus.edu.sg)

Sunil Kukreja is with SINAPSE, NUS and NASA, Armstrong Flight Research Center, CA 93524. (email: sunil.kukreja@mail.mcgill.ca)

Silvestro Micera is with Translational Neuro Engineering Lab, Center for Neuroprosthetics and Institute of Bioengineering, School of Engineering, École Polytechnique Fédérale de Lausanne (EPFL), Lausanne, Switzerland, and with the Biorobotics Institute, Scuola Superiore , Sant'Anna, Pisa, Italy (email: silvestro.micera@epfl.ch)

Martina Coscia is with the Biorobotics Institute, Scuola Superiore Sant'Anna, Pisa, Italy and with the Translational Neural Engineering Lab, Center for Neuroprosthetics and Institute of Bioengineering, School of Engineering, EPFL. (email: m.coscia@sssup.it)

Abhishek Mishra and Rohan Ghosh are with SINAPSE, NUS, 28 Medical Drive, #05-10, Singapore 117456. (email: abhishek.mishra@nus.edu.sg)

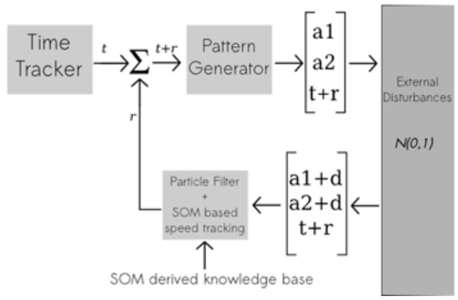


Fig. 1. A comprehensive view of the algorithm used to generate and maintain the locomotion. d is the small disturbance factor induced into the system by the environment, r is the time rate as perceived by the user and t is the base time generated by the time tracker. Simply stated, the algorithm iterates on values as decided by the current belief value.

Electromyographic (EMG) signals cannot be used effectively in this case [27], hence we use a force based model to simulate velocity change prediction. We show how a probabilistic state machine is helpful for this problem.

## II. Methods

### A. Data Collection

Normal patient data was obtained from the gait laboratory at the National University of Singapore (NUS) using a Vicon system. Markers were placed on the lower limbs at appropriate positions to generate kinematics data. Stroke data was collected at the Neuro-rehabilitation Unit Ospedale Cisanello Pisa, Italy. This clinical data is from 10 informed and willing patients (2 females and 8 males; Fugl-Meyer coefficients between 125 and 216).

### B. Gait Generation

In this model, gait is driven by using a pre-learnt basis pattern. The normative training data were obtained from the gait laboratory in NUS.

The SOM was trained on discrete values ranging from 1 to 198, using simple first order interpolation at non-integral points to make it continuous for controlling the joint velocity of exoskeleton. The following algorithm describes the procedure used for interpolation:

---

**Variables:**

$(a_1, a_2, t) \rightarrow$ *The hip-knee-time triplet vector, which describes the state of the leg*

$r \rightarrow$ *The time steps of the algorithm, which represents the relative speed at which the user walks (belief value)*

**Algorithm I:**

***1:*** *Given an observed state* $(a_1, a_2, t)$*, find the nearest SOM node* $\rightarrow n$ *and its distance from the observed state* $d_n$.

***2:*** *Find the distances of the* $(n+1)th$ *SOM node* $\rightarrow (d_{n+1})$ *and the* $(n-1)th$ *SOM node* $\rightarrow (d_{n-1})$ *from* $(a_1, a_2, t)$.

***3:*** $d_{min} = min(d_{n-1}, d_{n+1})$*, and index=SOM node value at lesser distance* $(n+1 \ or\ n-1)$.

***4:*** *The final SOM index of the observed state is given as:*

$$S(t) = \frac{index * d_n + n * d_{min}}{d_n + d_{min}} \tag{1}$$

---

### C. CPG and Repertoire Model

The CPG was designed as a feedforward neural network that interpolates the $(t+r)$ value at each step to its equivalent SOM node. This output was further processed by another neural network to produce a final output in vector format given as $\rightarrow (a1_{t=n}, a2_{t=n}, t=n)$. This neural network is compactly represented as :

$$\begin{gathered} node = net_1(t+r) \\ [a1, a2, t+r] = net_2(node) \\ t \in [1,198] \end{gathered} \tag{2}$$

$node$ is the current SOM node the CPG is at time $(t+r)$, $r$ is the belief value output by the particle filter based velocity control unit (see section II-E). In Eqn. 2, $r=1$ corresponds to normal gait velocity.

$net_1$ is a feedforward neural network that outputs the current SOM node which is further interpolated by $net_2$ to calculate the output vector values at $(t+r)$.

A Self-Organizing Map with 198 nodes was trained on $(a1, a2, t)$ values to generate the one dimensional representation. Two SOMs, one each for the left and the right leg were trained.

### D. Angular Constraints

To constrain gait output in the presence of measurement noise, a weighting factor $w$ was used to limit its effect as :

$$w_{new} = \{w_{old} * c\} + \{(1-c) * w_d\} \tag{3}$$

where, $w_{old}$ is the weighting factor value in the previous time sample ; $w_{new}$ is the weight factor value in the actual time sample, and $w_d$ is the disturbance weighting factor value, calculated as the ratio of the new and old hip joint angle values, and $w_d$ is updated at the next time sample as: $w_d \rightarrow w_{old}$

In equation 3, values of $c$ are in the closed interval from 0 to 1. A high c value permits our approach to be robust to measurement noise but with a cost of decreased sensitivity to subject movements. We used a low value of 0.2.

This weighting factor value was computed only in the healthy leg and its value was used for the affected leg. Thus, the affected leg is essentially the follower of the healthy leg. At time $(t+r)$, the output vector for healthy leg is calculated as $O_{t+r}$ and the effective output vector is updated as $O_{t+r} \rightarrow O_{t+r} * w_{new}$.

### E. Velocity Control using Probability Based Particle Filter

The goal of the particle filter is to finely modulate the walking speed following the user's intention , by considering the deviations from the predicted normal gait. Please note that we use the terms particle filter and probabilistic machine interchangeably throughout the paper to refer to the modified particle filter algorithm used. In the algorithm used for gait velocity prediction, the state of a leg is described by $a_1$, $a_2$ and t. Variable t represents the time normalized by T, where T is the time period of one full gait cycle at normal

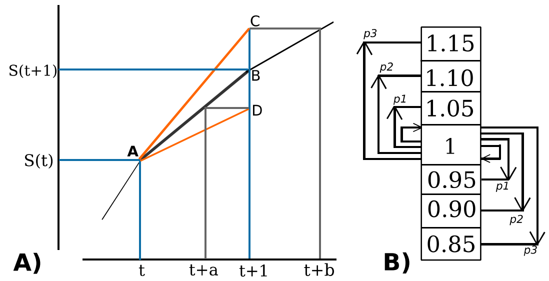


Fig. 2. (A) Line AB is the expected path taken by the SOM indices (base velocity line), whereas the lines AC and AD show the cases where there are deviations from the normal velocity. In case of AD, the timestep has effectively decreased as indicated by its extrapolation on AB. Similarly, there is an increase of the same parameter in case of path AC. In case of AD, the velocity has decreased while in case of AC, the velocity will increase. (B) This figure shows the probability based particle filter model used showing transitions from normal walk velocity state to the other states. The model is symmetric with respect to direction (back and forth).

speed. The gait data in one dimensional form, as represented by the SOM indices is used to compute the velocity. The index of the SOM weights is represented at time t with $S(t)$, where $S(t)$ is a continuous scalar variable varying from 1 to $N$, and $N$ is the total number of neurons used in the SOM ($N = 198$). $S(t)$ is obtained through the leg state tuple - $(a_1, a_2, t)$, using algorithm I. The index of the state observed at time $t+1$ could be either higher or lower than $S(t+1)$, as depicted by lines AC and AD as shown in Fig. 2. In the case when the observed state at time $t+1$ gives an index $O(t+1)$, which is lower than $B \leftrightarrow S(t+1)$, the relative time step is obtained by drawing a line parallel to the time axis and passing through $O(t+1)$ *or* $D$. In Fig. 2, t+a is the time point when this line intersects the curve. The new predicted speed is given by $a$. This value that is also related to the probabilities contained within the algorithm. In the same manner, if $O(t+1)$ is greater than $S(t+1)$ or C, the new time step is $b$. This value is higher than $r = 1$, indicating a higher walking speed. Thus, at each time instance, the system variables include $r$, the current predicted speed or the current rate at which the person is walking, and state of the leg at time t. For each observation, $r$ is updated by the particle filter like system. Each state of the particle filter is indicated by a number $R(i)$, which is representative of the relative rate at that node. A probability $P(i)$ is associated to each state, such that the sum of transition probabilities is 1. When the system is initialized, all the probabilities lie within the state in the middle, characterized by an $r$ value of 1. The transition probability $T_{ij}$ of $S_i$ ($ith$ state) to $S_j$ is given as:

$$T_{ij} = \frac{C}{\left(1 + abs(i-j)\right)^2} \tag{4}$$

By using a transformation matrix based on the Gaussian probability propagation, the equation 4 becomes:

$$T_{ij} = C.\mathrm{e}^{\left(-\frac{(i-j)^2}{D}\right)} \tag{5}$$

Parameter $D$ is the variance, and $C$ is fixed for a particular state $S_i$. $C$ can be obtained by normalizing the probabilities.

As with particle filter systems, the transition probability matrix is used to update the probabilities $P(i)$, and by adding the new observation $O(t+1)$, to find the instantaneous rate $r$ (belief value as defined earlier, also called the relative user velocity). The updated P(i) is obtained by centering a Gaussian on $r$ and multiplying the values thus generated by the function at the state of the particle filters with P(i). The new prediction after normalization is computed by the following equation:

$$r = \sum_{i=1}^{M} P(i)R(i) \tag{6}$$

This value is the new time step or rate in the algorithm. At the next iteration, the observation at time t+2 is then represented by $O(t+r)$, since the $r$ value was initially one. Similarly, the straight line between $S(t)$ and $S(t+1)$ is replaced by $S(t+a)$ and $S(t+a+r)$. This loop is iterated after each observation, and the probabilities and transition matrix are updated before each transition. A point to be noted is that the observation frequency does not change, and therefore, the system is always observed at discrete intervals of $T_s$. In addition, $r$ represents an overall phase velocity of the system, as the algorithm moves from $t$ to $t+r$ in each iteration. Finally, a summary of this algorithm is presented below:

---

**Variables:**

$(A, B) \rightarrow$ *The lower and upper time limit for the observations. Initially,* $A \rightarrow 1$, $B \rightarrow 2$, *and* $r \rightarrow 1$. *The relationship between these value is* $B = A + r$.

$R(i) \rightarrow$ *Describes the relative rate of the* $ith$ *state in the particle filter system.*

$P(i) \rightarrow$ *Set of probabilities for the ith state of the system. Initially,* $P(i) \rightarrow 1\, for\ i\ where\ R(i) \rightarrow 1$.

$T_{ij} \rightarrow$ *Probability transition matrix*

**Algorithm II:**

***1:*** $S(A)$ *is the SOM index pertaining to the previous observation, at time t, and* $S(A+r)$ *(at time t+1) is obtained by extrapolation using the slope at A.*

*2:* $O(A+r)$ *is the observation at time t+1, which maps to the relative time* $a$.

*3: The transition matrix* $T_{ij}$ is used *to update the probabilities.*

*4: A Gaussian is centered at* $a$*, multiplying the values at the points represented by* $R(i)$*, to obtain the new values of probabilities as :*

$$P(i) = C \times R(i) \times G\big(R(i)\big) \tag{7}$$

$C$ *is obtained by normalizing* $P(i)$.

***5****: The relative rate of the system r is computed.*

*6: A is updated as* $A + a$*, B as* $A + a + r$*, and the process is iterated.*

---

TABLE I
STROKE PATIENT DATA

| Months Since Stroke | Side Hemiplegic | Stroke Type | Fugl-Meyer |
|---|---|---|---|
| 60 | Left | Hemorrhagic | 160 |
| 27 | Left | Hemorrhagic | 125 |
| 49 | Left | Ischemic | 132 |
| 61 | Right | Hemorrhagic | 127 |
| 40 | Left | Ischemic | 130 |
| 8 | Right | Hemorrhagic | 160 |
| 48 | Left | Ischemic | 147 |
| 39 | Left | Ischemic | 141 |
| 63 | Left | Ischemic | 216 |
| 222 | Left | Hemorrhagic | 206 |

## III. RESULTS

The gait data for healthy patients was smoothed using a six-term Fourier series function given by:

$$f(x) = a_0 + \sum_{i=1}^{6} \left( (\alpha_i \sin(i.f.x)) + (\beta_i \cos(i.f.x)) \right) \quad (8)$$

The simulations were performed using MATLAB (MathWorks Inc.). It is to be noted that in all simulations, the left leg is assumed affected while the right leg is healthy. Any change in the velocity of the system was initiated by the user by a force on the healthy leg, changing the belief of the particle filter backend.

In all simulations, a Gaussian noise with standard deviation = 0.1 was added to the environment.

$$S_o = S_a + N(0,0.1) \quad (9)$$

$S_o$ is the observed SOM node and $S_a$ is the actual SOM node.

In the first simulation, the velocity of the healthy leg followed a sine waveform to assess its ability to control the affected leg using our technique. The results of this study are shown in the Fig. 3A.

In the next simulation, the user's intended velocity was kept constant at 0.8 and the system was initialized to have a prior belief value of 1 (r=1). Fig. 3B illustrates the time required to converge to 0.8, with a Gaussian noise of standard deviation 0.1 applied to it.

Fugl-Meyer factor is an important quantitative and physiotherapic measure of the amount of recovery in a patient after hemiplegia. The aim of any rehabilitative task is promoting the usage of the affected limb to speed and aid the brain to recover neural control of the limb. A robotic exoskeleton should therefore not only provide for the necessary locomotive support but also facilitate recovery by promoting the use of the affected limb in an appropriate manner [6, 28-33].

To this end, we propose the following modification to the exoskeleton algorithm. We choose an appropriate membership function $m(x)$ to calculate the value of the recovery factor $R$, given the Fugl-Meyer assessment parameter denoted by $\gamma$. Hence,

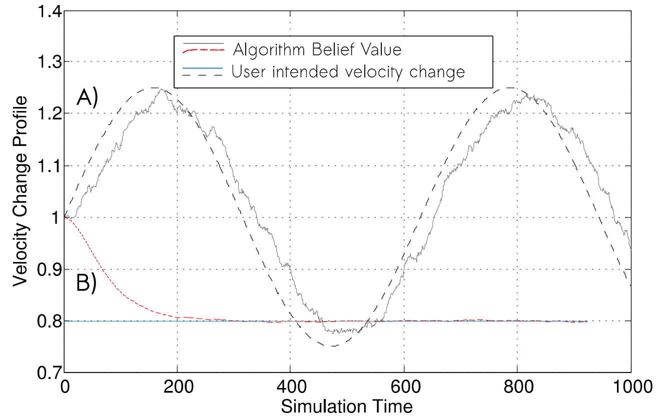


Fig. 3. (A) A Gaussian noise of standard deviation 0.1 was applied on the affected leg as an observation error to see the belief change of the particle system. (B) The belief propagation and convergence of the algorithm for velocity of the affected leg (dotted line) vs. velocity of the healthy leg has been shown here. A Gaussian noise was added on the observed rate. The healthy leg started with a velocity of 0.8 while the initial belief of the particle filter was r=1.

$$\begin{gathered} R = m(\gamma) : \gamma \in [0,226]\,, R \in [0,1] \\ m(\gamma = 0) = R_0 = 0 \\ m(\gamma = 226) = R_{226} = 1 \end{gathered} \quad (10)$$

Angles exhibited by the affected leg are attenuated with respect to correct values mirrored in the healthy counterparts. Thus, we relate the stroke affected angular velocity $[\dot{\theta_p}]$ to the correct $[\dot{\theta_e}]$ using a simple multiplicative model as shown:

$$K = \frac{\dot{\theta_p}}{\dot{\theta_e}} = \frac{\int_0^T \tau_p dt}{\int_0^T \tau_e dt} \quad (11)$$

The integral form is stated for clarity since the exoskeleton sensors give torque output at discrete time intervals. The behavior and distribution of $K$ was investigated using the

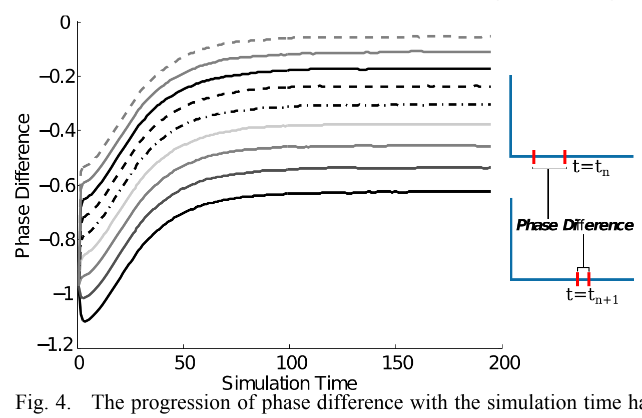


Fig. 4. The progression of phase difference with the simulation time has been shown here for $\mu$ values from 0.1 to 0.9 (top to bottom). It can be seen how higher of control given to a user ($\mu$=0.9) can result in a large phase difference between the legs. Hence, an optimum $\mu$ value must be chosen such that the tradeoff between this final phase difference and rehabilitation exercise remains optimum. The small figure on the right depicts how the affected leg gradually reaches to a smaller phase difference. The two bars represent angular values on the y axis. In an ideal case ($\mu$=0), the two bars will always coincide and there will be no phase difference. The left bar (affected leg marker) moves at a different velocity than the healthy leg based on the probabilistic state machine belief, and eventually catches up with some small phase lag.

stroke patient data available. We comment on the distribution of $K$ being approximated as $N(\mu, \sigma)$.

Let the correct torque to be applied to a joint by the exoskeleton to move the affected foot during the time interval $t$ to $t + T_s$, be denoted by $\tau_e$. If complete control is given to the exoskeleton, the patient would not need to exert any force on the affected leg, rendering the rehabilitation exercise to be of little value. To facilitate successful rehabilitation of patient, we leave out a part of $\tau_e \to \mu\tau_e$, to the patient. Hence, the total torque to the exoskeleton for the time period $T_s$ is :

$$\tau_{total} = (1-\mu)\tau_e + \mu\tau_p \tag{12}$$

Where $\tau_p$ is the incorrect torque applied by the patient to the stroke-affected leg. The net angular displacement of a joint in time $T_s$ is :

$$\begin{gathered} \Delta\theta_t = CT_s^2\tau_{total}(t) + \dot{\theta}_t T_s = CT_s^2\tau_{total}(t) + (\theta_t - \theta_{t-T_s}) \\ \Delta\theta_t = \theta_{t+T_s} - \theta_t \\ \Delta\ddot{\theta}_t = \theta_{t+T_s} - 2\theta_t + \theta_{t-T_s} \\ [\ddot{\theta}_t] = CT_s^2\tau_{total}(t) \end{gathered} \tag{13}$$

Without loss of generality, we assume $\dot{\theta}_0$ and $\theta_0$ to be zero.

$$[\dot{\theta_t}] = \sum_{n=1}^{\frac{t}{T_s}} CT_s^2\tau_{total}(nT_s) \tag{14}$$

From (13) and (14), we have:

$$[\dot{\theta}_t] = \sum_{n=1}^{\frac{t}{T_s}} \left( CT_s^2(1-\mu)\tau_e(nT_s) + CT_s^2\mu\tau_p(nT_s) \right)$$

$$= (1-\mu)[\dot{\theta_e}] + \mu[\dot{\theta_p}]$$

$$= \left[\dot{\theta}_e\right](1 - \mu + \mu K)$$

We observe that only a part of the angular velocity is mirrored onto the affected leg. Thus, we can equivalently hypothesize the same for absolute velocities recorded by the SOM based framework. Therefore we have:

$$[v_t] = [v_e]\big(1 - \mu(1-K)\big) \tag{15}$$

where $[v_t]$ and $[v_e]$ are the mirrored affected leg and the healthy leg velocity, respectively. This velocity is not the absolute velocity of the subject's center of mass; it is the rate at which the complete state of the system described by the gait angles change. The phase velocity belief as computed by our algorithm is independent of this ratio, since it is only dependent on the observed speed and the particle filter. This ratio signifies the inability of the partially human controlled exoskeleton to reach the current phase of the healthy leg. If $\varphi(t)$ is the phase of the healthy leg as observed at $t$, and $\psi(t)$ is the phase of the affected leg at $t$, then at $t + T_s$, $\psi(t)$'s movement is restricted by the parameter $\mu$ as follows:

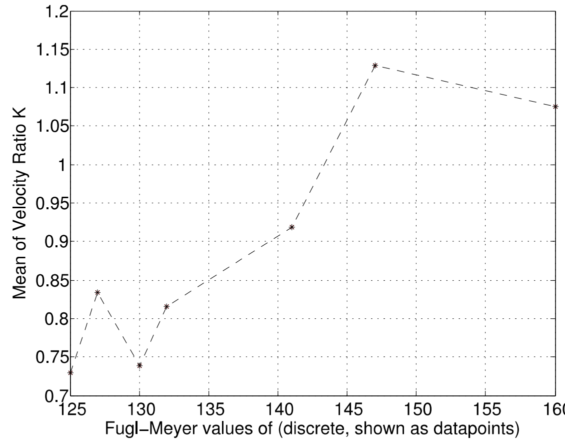


Fig. 5. This figure shows the mean of the velocity ratios for each Fugl Meyer value.

$$\psi(t+T_s) = \\ \big(\varphi(t) + r - \psi(t)\big)(1 - \mu + \mu K) + \psi(t) \tag{16}$$

If no control is given to the subject ($\mu = 0$), then $\psi(t + T_s) = \varphi(t) + r$, which is the same as for the normal case.. Hence, for non-zero $\mu$, the phase difference between the two legs takes more time to converge.

The value of the parameter $K$ was found to be centered about a mean that varies with respect to different patients as shown in Fig. 5. The results show that patients with high Fugl-Meyer values generally exhibit higher mean values, and less noise, with the value converging towards 1 at full recovery.

## IV. Discussions and Conclusions

The algorithm described in this study successfully produced the required pattern from a pre-learnt behavior. We showed that our technique is capable of maintaining a stable limit cycle in the presence of noise while simultaneously following (localizing) the patient's intended velocity of motion.

Understanding the intention of the patient is an important topic of research. In this study, we have shown a simple model to localize the intention of the user for changing gait velocity using a state machine. This method can be developed further to perform better prediction.

In unilateral stroke, the kinematics and muscle activity (particularly the proximal muscles) of the unaffected side also shows deviations. This is due to the fact that gait is controlled by modular muscle synergies controlling both legs [34]. However, we have not taken this into account and assumed that with the correction provided by the robotic exoskeleton, the healthy leg will follow a normal gait profile. In Fig. 3A, a uniform delay can be observed between the user's intended speed and the system's belief $r$. Two parameters that influence this delay are:

a) The transition probability $T_{ij}$; by increasing the variance, the time required for the algorithm to converge to the user's intended velocity is higher, and increases the delay.

b) The $r$ value of the particle filter states $S_i$ range from 0.5 to 1.5.

This delay has an inevitable tradeoff with respect to the noise produced by the particle filter belief. Other localization techniques such as Kalman filters can be applied in this case to improve the performance of the algorithm. The particle filter used here works on the associated probabilities of each state unlike its conventional use. This helps in faster computation as probability propagation can be realized through simple matrix manipulations unlike the conventional case where each particle needs to be updated.

## REFERENCES


[1] J. M. Belda-Lois, S. Mena-del Horno, I. Bermejo-Bosch, J. C. Moreno, J. L. Pons, D. Farina, M. Iosa, M. Molinari, F. Tamburella, A. Ramos, A. Caria, T. Solis-Escalante, C. Brunner, and M. Rea, "Rehabilitation of gait after stroke: a review towards a top-down approach," *J Neuroeng Rehabil,* vol. 8, p. 66, 2011.

[2] M. A. Dimyan and L. G. Cohen, "Neuroplasticity in the context of motor rehabilitation after stroke," *Nat Rev Neurol,* vol. 7, pp. 76-85, Feb 2011.

[3] T. H. Murphy and D. Corbett, "Plasticity during stroke recovery: from synapse to behaviour," *Nat Rev Neurosci,* vol. 10, pp. 861-72, Dec 2009.

[4] S. L. Small, G. Buccino, and A. Solodkin, "Brain repair after stroke--a novel neurological model," *Nat Rev Neurol,* vol. 9, pp. 698-707, Dec 2013.

[5] A. Chase, "Neural repair and rehabilitation: new assistive devices for stroke rehabilitation," *Nat Rev Neurol,* vol. 10, p. 59, Feb 2014.

[6] F. D. Shelton, B. T. Volpe, and M. Reding, "Motor impairment as a predictor of functional recovery and guide to rehabilitation treatment after stroke," *Neurorehabil Neural Repair,* vol. 15, pp. 229-37, 2001.

[7] H. Wood, "Stroke. a new window of opportunity for stroke rehabilitation?," *Nat Rev Neurol,* vol. 7, p. 4, Jan 2011.

[8] W. H. Chang and Y. H. Kim, "Robot-assisted Therapy in Stroke Rehabilitation," *J Stroke,* vol. 15, pp. 174-181, Sep 2013.

[9] L. W. Forrester, A. Roy, R. N. Goodman, J. Rietschel, J. E. Barton, H. I. Krebs, and R. F. Macko, "Clinical application of a modular ankle robot for stroke rehabilitation," *NeuroRehabilitation,* vol. 33, pp. 85-97, 2013.

[10] G. Grimaldi and M. Manto, "Functional impacts of exoskeleton-based rehabilitation in chronic stroke: multi-joint versus single-joint robotic training," *J Neuroeng Rehabil,* vol. 10, p. 113, 2013.

[11] S. Hesse, J. Mehrholz, and C. Werner, "Robot-assisted upper and lower limb rehabilitation after stroke: walking and arm/hand function," *Dtsch Arztebl Int,* vol. 105, pp. 330-6, May 2008.

[12] Y.-w. Hsieh, K.-c. Lin, C.-y. Wu, H.-y. Lien, J.-l. Chen, C.-c. Chen, and W.-h. Chang, "Predicting Clinically Significant Changes in Motor and Functional Outcomes After Robot-Assisted Stroke Rehabilitation," *Archives of Physical Medicine and Rehabilitation,* vol. 95, pp. 316-321, 2// 2014.

[13] S. Masiero, P. Poli, G. Rosati, D. Zanotto, M. Iosa, S. Paolucci, and G. Morone, "The value of robotic systems in stroke rehabilitation," *Expert Rev Med Devices,* vol. 11, pp. 187-98, Mar 2014.

[14] C. Werner, S. Von Frankenberg, T. Treig, M. Konrad, and S. Hesse, "Treadmill training with partial body weight support and an electromechanical gait trainer for restoration of gait in subacute stroke patients: a randomized crossover study," *Stroke,* vol. 33, pp. 2895-901, Dec 2002.

[15] D. Aoyagi, W. E. Ichinose, S. J. Harkema, D. J. Reinkensmeyer, and J. E. Bobrow, "A robot and control algorithm that can synchronously assist in naturalistic motion during body-weight-supported gait training following neurologic injury," *IEEE Trans Neural Syst Rehabil Eng,* vol. 15, pp. 387-400, Sep 2007.

[16] S. Jezernik, G. Colombo, and M. Morari, "Automatic gait-pattern adaptation algorithms for rehabilitation with a 4-DOF robotic orthosis," *Robotics and Automation, IEEE Transactions on,* vol. 20, pp. 574-582, 2004.

[17] H. Schmidt, S. Hesse, R. Bernhardt, J\, \#246, r. Kr\, \#252, and ger, "HapticWalker---a novel haptic foot device," *ACM Trans. Appl. Percept.,* vol. 2, pp. 166-180, 2005.

[18] S. K. Banala, K. Seok Hun, S. K. Agrawal, and J. P. Scholz, "Robot Assisted Gait Training With Active Leg Exoskeleton (ALEX)," *Neural Systems and Rehabilitation Engineering, IEEE Transactions on,* vol. 17, pp. 2-8, 2009.

[19] A. Mishra, S. Huang, Y. Haoyong, and N. V. Thakor, "Bipedal locomotion modeled as the central pattern generator (CPG) and regulated by self organizing map for model of cortex," in *Point-of-Care Healthcare Technologies (PHT), 2013 IEEE*, 2013, pp. 50-53.

[20] R. M. Harris-Warrick, "General principles of rhythmogenesis in central pattern generator networks," *Prog Brain Res,* vol. 187, pp. 213-22, 2010.

[21] M. MacKay-Lyons, "Central pattern generation of locomotion: a review of the evidence," *Phys Ther,* vol. 82, pp. 69-83, Jan 2002.

[22] E. Marder and D. Bucher, "Central pattern generators and the control of rhythmic movements," *Curr Biol,* vol. 11, pp. R986-96, Nov 27 2001.

[23] T. Kohonen, "Self-organized formation of topologically correct feature maps," *Biological Cybernetics,* vol. 43, pp. 59-69, 1982/01/01 1982.

[24] J. H. Kotecha and P. M. Djuric, "Gaussian sum particle filtering for dynamic state space models," in *Acoustics, Speech, and Signal Processing, 2001. Proceedings. (ICASSP '01). 2001 IEEE International Conference on*, 2001, pp. 3465-3468 vol.6.

[25] J. H. Kotecha and P. M. Djuric, "Gaussian particle filtering," *Signal Processing, IEEE Transactions on,* vol. 51, pp. 2592-2601, 2003.

[26] R. van den Brand, J. Heutschi, Q. Barraud, J. DiGiovanna, K. Bartholdi, M. Huerlimann, L. Friedli, I. Vollenweider, E. M. Moraud, S. Duis, N. Dominici, S. Micera, P. Musienko, and G. Courtine, "Restoring voluntary control of locomotion after paralyzing spinal cord injury," *Science,* vol. 336, pp. 1182-5, Jun 1 2012.

[27] B. Cesqui, P. Tropea, S. Micera, and H. I. Krebs, "EMG-based pattern recognition approach in post stroke robot-aided rehabilitation: a feasibility study," *J Neuroeng Rehabil,* vol. 10, p. 75, 2013.

[28] J. L. Crow and B. C. Harmeling-van der Wel, "Hierarchical properties of the motor function sections of the Fugl-Meyer assessment scale for people after stroke: a retrospective study," *Phys Ther,* vol. 88, pp. 1554-67, Dec 2008.

[29] P. W. Duncan, M. Propst, and S. G. Nelson, "Reliability of the Fugl-Meyer assessment of sensorimotor recovery following cerebrovascular accident," *Phys Ther,* vol. 63, pp. 1606-10, Oct 1983.

[30] D. J. Gladstone, C. J. Danells, and S. E. Black, "The fugl-meyer assessment of motor recovery after stroke: a critical review of its measurement properties," *Neurorehabil Neural Repair,* vol. 16, pp. 232-40, Sep 2002.

[31] J. Sanford, J. Moreland, L. R. Swanson, P. W. Stratford, and C. Gowland, "Reliability of the Fugl-Meyer assessment for testing motor performance in patients following stroke," *Phys Ther,* vol. 73, pp. 447-54, Jul 1993.

[32] J. See, L. Dodakian, C. Chou, V. Chan, A. McKenzie, D. J. Reinkensmeyer, and S. C. Cramer, "A standardized approach to the Fugl-Meyer assessment and its implications for clinical trials," *Neurorehabil Neural Repair,* vol. 27, pp. 732-41, Oct 2013.

[33] K. J. Sullivan, J. K. Tilson, S. Y. Cen, D. K. Rose, J. Hershberg, A. Correa, J. Gallichio, M. McLeod, C. Moore, S. S. Wu, and P. W. Duncan, "Fugl-Meyer assessment of sensorimotor function after stroke: standardized training procedure for clinical practice and clinical trials," *Stroke,* vol. 42, pp. 427-32, Feb 2011.

[34] P. Tropea, V. Monaco, M. Coscia, F. Posteraro, and S. Micera, "Effects of early and intensive neuro-rehabilitative treatment on muscle synergies in acute post-stroke patients: a pilot study," *J Neuroeng Rehabil,* vol. 10, p. 103, 2013.